Eur Biophys J (2001) 30: 198–206
DOI 10.1007/s002490100139

ARTICLE

Assen Koumanov · Normann Spitzner · Heinz Rüterjans
Andrey Karshikoff

Ionization properties of titratable groups in ribonuclease T_1

II. Electrostatic analysis

Received: 22 August 2000 / Revised version: 21 December 2000 / Accepted: 21 December 2000 / Published online: 20 March 2001

Abstract The experimental NMR data for the individual titratable groups in ribonuclease T_1 presented in the preceding paper were analysed by means of a continuum dielectric model. The role of two factors, the alteration of hydrogen loci on the ionizable groups and the conformational flexibility, were analysed. It was suggested that the position of the titratable hydrogen is essential mainly for strongly interacting groups. For groups which are accessible to the solvent and whose ionization is not coupled with the ionization of neighbouring groups, this factor can be neglected. The influence of the conformational flexibility on the electrostatic interactions becomes apparent for the environment of K25. For some strongly interacting groups, non-sigmoidal ionization curves were calculated. On this basis the pH dependence of the NMR chemical shift of the $^{13}C\epsilon^2$ resonance of H27, whose ionization is coupled with E82, was reproduced.

Keywords Proteins · Ionization · Ribonuclease T_1 · Electrostatic interactions · pK_a

Introduction

Functional properties of proteins are a result of a fine balance of non-covalent interactions. Among them, electrostatic interactions play a role, which becomes evident at any pH-dependent property. Protonation/deprotonation equilibria of titratable side chains may cause changes of the electrostatic potential and in this way contribute to, for instance, protein-substrate interactions, induce conformational changes and regulate enzymatic activity. A well-known example for a pH-controlled functional property of proteins is the Bohr effect in hemoglobin. That is why electrostatic interactions are in the scope of the interest of a large community of researchers.

Kirkwood and Tanford (Kirkwood 1934; Tanford and Kirkwood 1957) developed a theory for the treatment of electrostatic interactions in proteins which was one of the main tools for computation of the electrostatic properties of proteins for a long period. Several different approaches for calculation of the electrostatic interactions in proteins have been proposed in the last two decades. The most rigorous one is the microscopic model proposed by Warshel (Warshel 1981; Warshel and Russell 1984). In this approach, the problem is treated at the atomic level by explicit consideration of the partial charges and polarizabilities in the system. In many cases, computationally more convenient is the macroscopic approach, where the protein molecule is treated as a microphase with a low dielectric constant immersed in a high permittivity medium. In fact, this is an extension of the Kirkwood theory (Kirkwood 1934); however, the position of the charges, as well as the irregularity of the dielectric interface are taken into account. For this system, the Poisson-Boltzmann equation is solved numerically. First Warwicker and Watson (1982) proposed a rational method for solving the Poisson-Boltzmann equation for proteins by means of finite difference integration. It has been further developed (Klapper et al. 1986; Nicholls and Honig 1991) and nowadays it is probably one of the most popular computational techniques. Other successful methods can be mentioned, such as the generalized Born model (Srinivasan et al. 1999); for a review see also Ullmann and Knapp (1999). All these model assumptions point to one and the same problem, namely, the determination of the charge state of the titratable groups at a given pH. The exact solution of this problem has been proposed by

A. Koumanov · A. Karshikoff (✉)
Karolinska Institute, Department of Biosciences at Novum,
141 57 Huddinge, Sweden
E-mail: aka@csb.ki.se
Tel.: +46-8-6089180
Fax: +46-8-6089179

N. Spitzner · H. Rüterjans
Institute of Biophysical Chemistry,
Johann Wolfgang Goethe University,
Marie-Curie-Strasse 9, 60439 Frankfurt a.M., Germany

Bashford and Karplus (1990), who developed a statistical mechanical method for calculation of the probability of a given titratable group to be in its protonated or deprotonated state. Another problem that has to be solved is the evaluation of the role of protein conformational flexibility. There is a number of examples showing that small conformational changes can have an essential influence on the ionization of the titratable groups (Karshikoff 1995; Berisio et al. 1999; Nakasako et al. 1999). In principle, there are no theoretical obstacles for including conformational diversity into the calculations. Alexov and Gunner (1997, 1999) have proposed a procedure for incorporating of conformational flexibility which is limited to the variance of titratable proton location. Spassov and Bashford (1999) have elaborated a complete theoretical approach for calculation of electrostatic interactions where conformational flexibility as well as variance of titratable proton locations are taken into account. However, as these authors point out, the complexity of the problem becomes prohibitively large if these two factors are considered.

The magnitude of electrostatic interactions in proteins cannot be directly measured; therefore, their theoretical prediction is of key importance for the analysis and understanding of a variety of protein properties. Fortunately, the ionization curves of the titratable groups in proteins in principle can be detected experimentally. NMR provides one of the most reliable experimental observations of ionization behaviour of individual titratable sites in proteins. As far as NMR is sensitive to the changes of the environment of the monitoring nuclei, the observed titration curve reflects both proton release (or binding) and possible conformational changes that may take place upon changing pH. There are plenty of examples in the literature for pH dependencies of the chemical shift with more than one inflection or adopting a dome-like shape. In the preceding paper we also demonstrated an unusual titration of several groups of RNase T_1. Obviously, such titration curves reflect all factors mentioned above: the conformational diversity, a variance of titratable proton locations, as well as the cooperative ionization of titratable groups.

Here, we continue with the theoretical analysis of the experimentally observed titration curves presented in the preceding paper. We focused on the peculiar titration of some groups in RNase T_1 and tried to give an interpretation. For instance, we showed that the complex titration of H27 is a result of the strong electrostatic coupling, including hydrogen bond formation of this residue with E82. The role of the conformational flexibility and the hydrogen positions on the titratable sites are discussed.

Methods

The computational procedure used in this work does not differ essentially from that described earlier (Karshikoff 1995). It was assumed that only electrostatic interactions contribute to the ionization properties of the titratable groups. In this way, the protonation free energy ΔG_i of the ith group is:

$$\Delta G_i = RT \ln 10(\mathrm{pH} - \mathrm{p}K_\mathrm{m}) + \Delta G_{i,\mathrm{el}} \tag{1}$$

where $\mathrm{p}K_\mathrm{m}$ refers to the standard free protonation/deprotonation equilibrium of a model amino acid residue in solution corresponding to a particular type, m, of titratable groups. The correction term:

$$\Delta G_{i,\mathrm{el}} = \Delta G_{i,\mathrm{sol}} + \Delta G_{i,\mathrm{pc}} + \Delta G_{i,\mathrm{tc}} \tag{2}$$

which is the subject of calculations, comprises the contribution of the desolvation penalty, $\Delta G_{i,\mathrm{sol}}$, the interaction of the ith group with the protein permanent charges, such as partial atomic charges of the polar groups and peptide chain, $\Delta G_{i,\mathrm{pc}}$, and the contribution of electrostatic interactions with all other titratable groups, $\Delta G_{i,\mathrm{tc}}$. Description of the calculations of these terms is given elsewhere (Karshikoff 1995). To keep consistency with the Tanford definition for intrinsic $\mathrm{p}K_\mathrm{a}$ (Tanford and Kirkwood 1957), the term $\Delta G_{i,\mathrm{tc}}$ was split into a term describing the work for charging the ith group if all other titratable sites are in their neutral form, $\Delta G_{i,\mathrm{tc(n)}}$, and a term, W_{ij}, counting for the change of this work if only the jth group is charged. The calculation of $\Delta G_{i,\mathrm{tc(n)}}$ is identical to that of $\Delta G_{i,\mathrm{pc}}$; however, protein permanent charges are replaced by partial charges of the titratable groups. Thus, one formally obtains an ionization energy term $\Delta G_{\mathrm{int},i}$ that at given pH depends only on the protein structure (i.e. on the situation of a given group in the protein) and does not depend on the charge-charge interactions between the titratable sites:

$$\Delta G_{\mathrm{int},i} = RT \ln 10(\mathrm{pH} - \mathrm{p}K_\mathrm{m}) + \Delta G_{i,\mathrm{sol}} + \Delta G_{i,\mathrm{pc}} + \Delta G_{i,\mathrm{tc(n)}} \tag{3}$$

The influence of charged titratable groups is counted by a matrix W_{ij} as follows:

$$W_{ij} = \sum_{k \in \{i\}} [(\varphi(j_\mathrm{c}, k) - \varphi(j_\mathrm{n}, k))(q_\mathrm{h}(k) - q_\mathrm{d}(k))] \tag{4}$$

where the sum is taken over all charged atoms, k, within group i. The quantities $\varphi(j_\mathrm{c}, k)$ and $\varphi(j_\mathrm{n}, k)$ are the electrostatic potentials created by the partial charges of group j in its charged and neutral form, respectively, and $q_\mathrm{h}(k)$ and $q_\mathrm{d}(k)$ are the partial charges of atoms k within the ith group in its protonated and deprotonated forms, respectively.

The fractional protonation θ_i of a titratable group at a given pH was calculated by means of the algorithm proposed earlier (Karshikoff 1995; Miteva et al. 1997). According to this algorithm, first the weakly interacting groups are selected and excluded from the statistical sum by means of a variant of the Tanford-Roxby procedure (Tanford and Roxby 1972). The statistical sum is then taken over the rest of the sites:

$$\theta_i = \sum_{\{x\}} x_i \mathrm{e}^{-\Delta G(x)/RT} \Bigg/ \sum_{\{x\}} x_i \mathrm{e}^{-\Delta G(x)/RT} \tag{5}$$

The summation is over all possible protonation states $\{x\}$, where $x = (x_1, x_2, \ldots x_i, \ldots x_S)$ is a vector of S elements corresponding to the number of sites included in the sum. Each element x_i adopts a value of 0 for the deprotonated or 1 for the protonated state of site i. The energy term $\Delta G(x)$ in the above sum has the form:

$$\Delta G(x) = \sum_i^S \left[x_i \Delta G_{\mathrm{int},i} + (Q_i + x_i) \left(\sum_{j \neq i}^S (Q_j + x_j) |W_{ij}|/2 + \sum_j^{TR} (Q_j + \theta_j) |W_{ij}| \right) \right] \tag{6}$$

where Q_i is the charge of group i in the deprotonated state. The last sum on the right-hand side of the above expression is taken over the set of weakly interacting groups ($S + TR$ gives the total number of titratable sites).

Two different computational schemes were used to calculate $\Delta G(x)$. The first one, scheme 1, employs an average charge distribution based on an assumption for equal representation of the possible positions of the titratable hydrogens. In the second one, scheme 2, calculations were performed by taking into account the combination of all possible positions of titratable hydrogen in the histidines and the carboxyl groups. Corresponding statistical weights were calculated by extending the statistical sum, adopting multiple neutral states of the above-mentioned groups. For the carboxyl groups, only the positions corresponding to a *cis* conformation of the O-CR-O-H group are considered (Fig. 1). This conformation is most populated for carboxylic acids in solution and determines the pK_m values. In order to reduce the computational time, *trans* conformations were omitted.

Parameters and input data

The protein molecule was represented as a medium with a dielectric constant of 4. A dielectric constant of 75 was taken for the surrounding solvent. This corresponds to a temperature of 35 °C (Hamer 1971) for which the experimental data were determined. Also, according to the experimental condition, an ionic strength of 0.03 was defined for the system. Partial atomic charges, as well as atomic radii, were taken from the Merck Molecular Force Field parameter set (Halgren 1996). To satisfy the limitations of the computational scheme 1, some charge values were appropriately changed. For the protonated state of the carboxyl groups and deprotonated states of the guanidines and imidazoles, the net charge of the hydrogens corresponding to these states was evenly distributed over all possible hydrogen locations. In the case of the deprotonated guanidines and protonated carboxyls, the charges of the corresponding heavy atoms were also averaged.

Finite difference calculations were performed in a grid box ($96 \times 96 \times 96$) with grid length of 0.64 Å. The calculations were followed by focusing (Klapper et al. 1986) on each titratable group with a grid size of 0.22 Å to calculate the desolvation energy, $\Delta G_{i,\mathrm{sol}}$. The final charge-charge interactions are calculated after focusing to a grid size of 0.43 Å, so that the entire molecule is in the grid box. X-ray coordinates of RNase T_1 (PDB code 9RNT) (Martinez-Oyanedel et al. 1991) were used in the calculations. In the case of multiple side-chain conformations, the conformers A were taken as a reference if nothing else was noted.

The values of pK_m used in the calculations are given in Table 1.

Results and discussion

The titration curves of all 29 ionizable groups in RNase T_1 were calculated employing both computational schemes. In order to facilitate the comparison with the experimental results, both experimental and calculated titration curves were fitted with the functions described in the preceding paper. Equation (2) from the preceding paper was used for the cases where standard deviation of the fit was less than 5% of the amplitude of the corresponding curves. For all other cases, Eq. (1) was used. This turned out to be a useful criterion for distinguishing the groups that strongly interact with the protein charge multipole. An important difference between the fitting of the experimental and the calculated data should be mentioned. The values of the chemical shift at the pH regions flanking the experimentally accessible interval are not fixed so that they were parameters of the fit, whereas the theoretical curves were fitted with fixed degrees of protonation for the extremes (1 and 0 at infinitely low and high pH, respectively). It must be noted that the inflections obtained by fitting of the calculated curves are not necessarily equivalent to $pK_{1/2}$. However, it can most certainly be applied for groups whose ionization is weakly coupled with the ionization of the other titratable groups. As far as this is the case for the majority of titratable groups, the inflections of the calculated ionization curves practically coincide with $pK_{1/2}$. For convenience, and to unify the terminology with the preceding paper, we will use the term pK_a to determine the pH value of the inflection point of a given ionization curve.

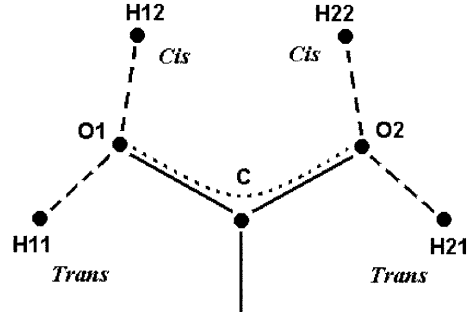

Fig. 1 Schematic representation of possible positions of a hydrogen in a carboxyl group in a protein. In positions H12 and H11 the hydrogen is covalently bounded to oxygen O1 and they are respectively in *cis* and *trans* conformation to oxygen O2 (O2-C-O1-H1x)

Table 1 Model pK_a values of the titratable groups used in the calculations

Group	pK_m [a]
N-terminus	8.2[b]
D	4.0
E	4.4
H	6.3
K	10.4
1R	12.0
Y	9.4
C-terminus	3.6[c]

[a] Data taken from Matthew (1985) and Bashford and Karplus (1990)
[b] pK_a of glycine amide (http://www.Science.smith.edu/Biochem/Biochem_353/Common_Buffers.htm)
[c] pK_a of *N*-acetylglycine (Hamer 1971)

Weakly interacting groups

The calculated and experimental pK_a values match relatively well (Table 2), which is typical for the fixed charge models. For weakly interacting groups, the calculations made according to schemes 1 and 2 produced similar pK_a values, which mainly results from the weak dependence of the desolvation energy on the proton position for these groups. The titratable protons are immersed in the van der Waals spheres of the heavy atoms, so that the low dielectric medium remains practically invariant in shape upon a change of proton

Table 2 pK_a values of titratable sites of RNase T_1

Site[a]	Experimental[b]	Calculated		
		Scheme 1	Scheme 2	H location[c]
Weakly interacting groups				
N-terminus	8.10[d]	9.31	9.31	–
D3	3.51	3.18	3.41	$O\delta^1$-H
Y4	–	12.38	12.38	–
Y11	–	> 13	> 13	–
D15	3.49	2.29	2.73	$O\delta^1$-H
Y24	–	> 13	> 13	–
E31	4.78	4.45	4.43	–
Y38		> 13	> 13	–
K41	8.6[e]	8.16	8.20	–
Y42	–	> 13	> 13	–
Y45	–	9.83[f]	9.83[f]	–
E46	3.58	4.34	4.35	–
D49	4.37	3.73	3.73	–
Y56	–	> 13	> 13	–
Y57	–	> 13	> 13	–
D66	3.89	3.87	3.83	–
Y68	–	12.26	12.26	–
E102	5.16	6.59	6.58	–
C-terminus		4.55	4.54	–
Strongly interacting groups				
H27	3.36	2.69	3.28	$N\delta^1$-H
	7.08	8.37	7.12	–
E82	3.24	3.24	3.53	–
	6.93	8.28	6.15	–
Active site				
H40	3.73	6.60	4.60	$N\epsilon^2$-H (40–80%)
	7.75	–	7.21	–
E58	3.93	< 1	< 1	–
D76	–[g]	6.45	6.71	$O\delta^1$-H
R77	–	> 13	> 13	–
H92	4.82	4.86	5.27	$N\epsilon^2$-H (60–95%)
	7.31	7.16	–	–

[a] pK_a values for K25, E28, and D29 are listed in Table 3
[b] pK_a values determined by NMR. Some values differ from those reported in the preceding paper because a different fitting procedure was used. In the case of the histidines, the pK_a values were derived from the pH dependence of the $^{13}C\epsilon^1$ resonance
[c] Hydrogen locations on titratable heavy atoms of histidines and carboxyl groups which were estimated by scheme 2. Only hydrogen location on carboxyl oxygens with predominating occupancy >90% are listed. If not indicated otherwise, the calculated distribution for all locations is within 40–60%
[d] Sample with phosphate (unpublished data)
[e] Iida and Ooi (1969)
[f] $pK_a > 13$ for B conformation of N99
[g] Ambiguous NMR data (see preceding paper)

location. This results in small deviations (below 0.3 kcal/mol) of the desolvation energy upon proton position alteration. In most cases there is a tendency of compensation due to an opposite change of the interactions with the protein environment (partial charges of the surrounding atoms). The majority of carboxyl groups showed a preferable distribution of the titratable hydrogens within 40–60% (Table 2). The pK_a values calculated for carboxyl groups with non-even occupancy of the titratable protons (scheme 2) were slightly shifted towards experimental values in comparison with values obtained with scheme 1.

The pK_a value calculated for K41 is unusually low (Table 2). According to the X-ray structure, the ϵ-amino group is deeply buried in the protein, which causes an essential increase of the desolvation penalty. This is supported by the results of Iida and Ooi (1969), who have also suggested a pK_a of 8.6 for one of the lysines in RNase T_1. A value of 11 has been calculated by Mehler (1996). This disagreement may arise from the different crystallographic data used in the calculations.

The pK_a values calculated for some groups differ from the experimental results. However, all of these groups are in conformations that most probably do not occur when the protein is in solution. Thus, for instance, the N-terminal chain is stretched out from the protein molecule, which leads to a low desolvation energy; therefore the calculated intrinsic pK_a remains close to the pK_m value. Although this site weakly interacts with other titratable groups, the high negative net charge of the molecule calculated for pH 8 shifts its pK_a up with about 1 pH unit. The NMR data (Pfeiffer et al. 1997) suggest an increased flexibility of this part of the molecule. Also, in all NMR models the N-terminal residue is closer to the protein part, in an environment favouring the deprotonated form. The difference between the calculated and the experimental pK_a seems to be related to the difference in the conformations that the N-terminal chain adopts in crystalline state and in solution. It will be demonstrated below that the pK_a value of the N-terminal amino group is very sensitive to the conformation of this part of the molecule. The pK_a values of E46 and D49 were calculated with the X-ray structure, which gives different conformations for these residues in comparison to NMR solution structures (Pfeiffer et al. 1997). Also, these residues were found to have an essential mobility of their side chain.

Another factor that may produce a discrepancy between the experimental and calculated pK_a values are the crystal contacts. The elevated pK_a value calculated for E102 is most likely due to a burial of this group in the protein interior, caused by the close contact to a neighbouring protein molecule in the crystal. A calcium ion is coordinated to the carboxyl group of D15 in the X-ray structure, which may cause a conformation of this residue different from that in solution. Also, most of the groups mentioned above are also involved in crystal contacts. Thus, two reasons can be given for the observed differences between the experimentally observed and the theoretically predicted pK_a values. Firstly, the crystal contacts may have an impact on the conformation of the side chains of the titratable groups. Secondly, the X-ray structure is determined at pH 7, which is far from the pH range where the carboxyl groups change their ionization state. It is possible that the conformations of side chains of these or neighbouring groups differ at low pH. One may also conclude that in spite of improving the predicted pK_a values by the introduction of the hydrogen loci distribution (scheme 2), the conformational distortions due to crystal contacts may have a dominant role. Thus, within the fixed charge model,

averaging of titratable proton charges for the weakly interacting groups can be used to reduce the complexity of the calculations.

Strongly interacting groups

H27 and E82 are a typical example of strongly interacting groups. The ionization curve calculated for H27 is shown in Fig. 2. It is characterized by a large plateau of the titration curve between pH 4 and pH 6, which separates two sigmoidal segments. Both computational schemes provided titration curves for H27 similar to the experimentally observed. Calculations with averaged charge distribution (scheme 1) produced a titration curve with two inflection points at pH 2.7 and pH 8.3 (see Table 2). The results obtained by scheme 2 match the experimental data much better. According to scheme 2, the deprotonation occurs primarily at $N\delta^1$, which is in a good agreement with the chemical shift of the $^{13}C\gamma$ resonance as a function of pH (see the preceding paper), also clearly indicating a predominant titration of the $N\delta^1$ atom of H27. The two inflection points at pH 7.1 and 3.4 in the experimental titration curve of the $^{13}C\epsilon^1$ resonance of H27 can be interpreted as pK_a values of two groups titrating at different pH ranges. Similarly, two pK_a values can be extracted from the titration curve of E82. These two sets of pK_a values practically coincide (Table 2), so that assignments of a pK_a of about 3.4 to E82 and a pK_a of 7.1 to H27 seem convincing.

The side chains of H40 and E58 form another strongly interacting couple. This pair is a member of a highly cooperative charge cluster – the active site charge cluster – comprising also D76, R77, and H92. Although the calculated pK_a values of H40 were not essentially different from the experimental values (see Table 2), the reproduction of some titration curves was not satisfactory. The calculation suggested a pK_a < 1 for E58 versus the experimental value of 4. Using another X-ray structure of RNase T1, Mehler (1996) has achieved an excellent agreement with the experimental data for this group. As already pointed out, the main source of this discrepancy is the limitation of the fixed charge model to one conformation. The NMR structure models show that this region of the molecule is characterized by a high flexibility (Pfeiffer et al. 1997). Most of the groups in this cluster can be found in a number of conformations, some of them essentially different from that found in the X-ray structure. In all NMR models, the imidazole ring of H40 was found to be flipped towards the X-ray structure.

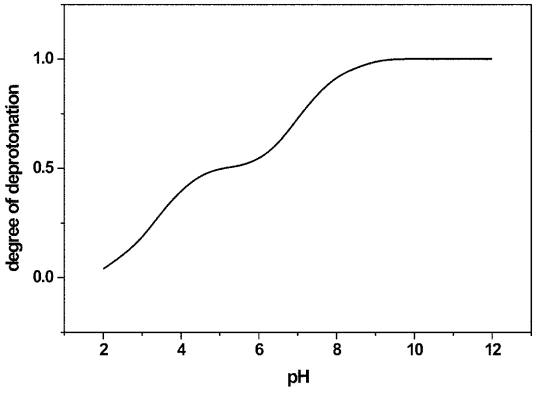

Fig. 2 Calculated ionization curve of H27 according to scheme 2

The conformational flexibility in this region seems also to be the main reason for pK_a values according to scheme 1, which are closer to the experimental data for H92. The titration curve can be fitted to the sum of two sigmoidal-shaped curves with inflections coinciding very well with the experimental pK_a values. However, the contribution of the sigmoidal curve with an inflection corresponding to a pK_a of 4.8 is 63% in disagreement with the presumed complete deprotonation, with a pK_a of 7.3 derived from the pH-dependent chemical shift data. Applying scheme 2, the probability for deprotonation of $N^{\delta 1}$ is pH dependent: 0.4 at pH 4 and 0.6 at pH 7. Obviously, in order to accurately reproduce the ionization of H92 and E58, conformational flexibility in this region has to be considered.

The ionization of D76 is another case of non-trivial titration. The chemical shift of this residue shows negligible pH dependence, with two hardly distinguishable inflections (see preceding paper). This most likely reflects a partial deprotonation of this residue. Based on a site-directed mutagenesis experiment, Giletto and Pace (1999) concluded that D76 has a pK_a of 0.5, which in fact is opposite to our result showing an extremely high pK_a value of 6.5 (see also Pfeiffer et al. 1998). Different factors strongly affect the ionization of this residue: (1) significant electrostatic interactions with active side residues R77 and H92; (2) a deeply buried carboxyl group; (3) several possible hydrogen bonds; and (4) the presence of bound water. While the impact of the first factor would favour a low pK_a value for D76, the second impact is clearly opposing a pK_a of 0.5 with apparent dominance of the high desolvation penalty stabilizing the protonated form. The presence of bound water and possible reorganization of the hydrogen bond network upon ionization are ambiguous with respect to the protonation/deprotonation equilibrium of this residue. These two factors are not fully considered in our computational model. They play probably the key role in achieving a relevant explanation of the contradiction among different experimental and theoretical studies.

The E28-K25-D29 triad

The difference between the experimental and theoretical pK_a values discussed above were addressed to differences in conformations in solution and in the crystalline state of the protein. Although this explanation is a speculative one and, on a qualitative level, in all cases discussed above were differences in conformations between the X-ray and NMR structures detected. The X-ray structure

of RNase T_1 used in the calculations also offers variation of side-chain conformation for a number of groups (T5, K25, L26, S35, K41, V78, and N99). We performed pK_a calculations for a combination of different conformations of these side chains. As expected, the conformational heterogeneity around or involving a titratable site influences the ionization equilibria essentially. Thus, for instance, the pK_a of Y45 changes from 9.8 to a value higher than 13 upon a change of the conformation of N99 from A to B. To our knowledge, there are no experimental data for Y45 to further analyse this result.

K25 is an interesting case. In conformation A, this residue forms a salt bridge with E28, whereas in conformation B it swaps its salt bridge partner to D29. In both conformations, K25 showed almost identical pK_a values. However, different pK_a values were obtained for the two alternative partners of this residue. Both computational schemes provide very similar results, so that in the following analysis only results obtained by scheme 2 will be used. The calculations showed that the pK_a values of E28 and D29 are in a good agreement with the experimental data for these conformations of K25, in which the corresponding carboxylate does not form a salt bridge. The pK_a values for the salt-bridged E28 and D29 are shifted to lower values (Table 3).

The occupancy of the two conformers of K25 in the X-ray structure is 1:1. We estimated this ratio by calculating the occupancy of conformations A and B as a function of pH. We assumed that van der Waals forces and interactions with the solvent do not differ significantly in the two conformations, so that only the electrostatic energy was considered. The probability of K25 to adopt one of two conformations was then calculated by:

$$p_i(\mathrm{pH}) = e^{-\Delta G_{\mathrm{el},i}(\mathrm{pH})/RT} \Big/ \sum_{i=1}^{2} e^{-\Delta G_{\mathrm{el},i}(\mathrm{pH})/RT} \qquad (7)$$

where i denotes the two lysine conformations and $\Delta G_{\mathrm{el},i}$ is the total electrostatic energy of all titratable sites for ith conformation. In the region of pH 7, which is the pH of crystallization, calculated occupancies were close to 1:1, which coincides with that observed in the crystal structure (see Fig. 3). At pH values below 7, conformation B appears to be more populated. This means that in the pH range where the titration of E28 and D29 are experimentally observed, the salt bridge K25-D29 is more populated. The ionization equilibria of E28 and D29 were calculated by taking into account the pH dependence of the population of K25 conformations. In Fig. 4 the titration curve of E28 is compared with the experimental data. The fit of the experimental data (see preceding paper) gives pK_a values of 3.9 and 5.6 with a contribution of 0.18 and 0.82, respectively. Applying the same procedure to the theoretical curve, one obtains pK_a values of 3.6 and 5.6 with contributions of 0.27 and 0.73, respectively. The contributions of the sigmoidal segments to both experimental and theoretical titration curves agree very well with the calculated distribution of the conformational occupancy of K25. One can conclude that the lower pK_a corresponds to conformation A (the low-populated salt bridge K25-E28), while the observed pK_a of 5.6 corresponds to the higher populated B conformation. The pK_a calculated for D29 in conformation B of K25 (i.e. when these groups form salt bridge) is about 1.5, which is out of the observable pH range. Most likely the observed pH dependence of the chemical shift of D29 corresponds to the low-populated conformation

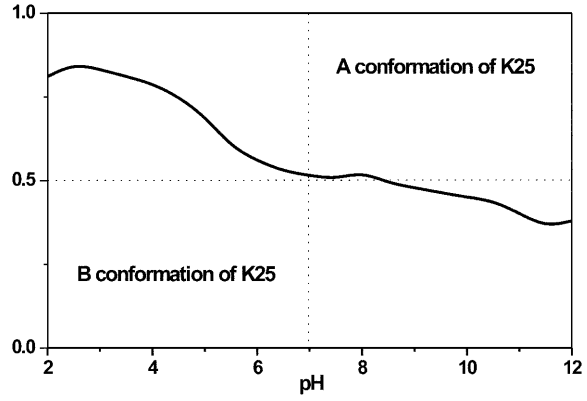

Fig. 3 Phase diagram of the X-ray conformers of K25. In the region of pH 7, which is the pH of crystallization, calculated populations A and B conformers of K25 are nearly equal, which coincides with the observed occupancies of 0.5 in the crystal structure

Table 3 pK_a values of D29, K25, and E28: experimental and calculated according to scheme 2 for A and B conformations of K25

Site	Experimental[a]	Calculated			
		Conformation A	H location[b]	Conformation B	H location[b]
D29	4.44	4.39	–	1.52	–
K25	–	12.84	–	12.41	–
E28	5.39	3.57	Oϵ^1-H	5.57	–

[a] pK_a values determined by NMR (see preceding paper)
[b] Only hydrogen location on carboxyl oxygens with predominating occupancy >90% are listed. If not indicated otherwise, the calculated distribution for all locations is within 40–60%

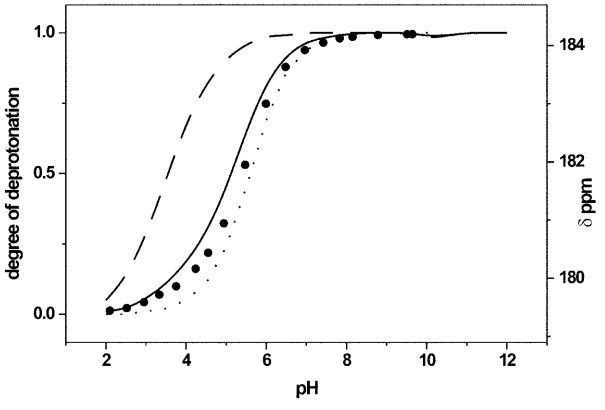

Fig. 4 E28 titration curve: (—) calculated by scheme 2, taking into account the population of the K25 conformations as a function of pH; (– – –) calculated for conformation A; (···) calculated for conformation B; (•) experimental data

A of K25. However, in that case, a smaller amplitude of the chemical shift should be expected.

The above speculations were made on the assumption that in solution RNase T_1 exists only in the two conformations (A and B) of K25 detected in the X-ray structure. The NMR solution structures (Pfeiffer et al. 1997) suggest that the side chain of K25 is flexible and adopts a variety of conformations, in which the ϵ amino group is far from the two possible salt bridge partners (see also Engelke and Rüterjans 1998). As seen from Table 3, the calculated pK_a values of E28 and D29 are in agreement with the experimental ones if any of these groups does not form a salt bridge with K25. This gives rise to another interpretation of the experimental data, namely that the K25 conformations A and B are less populated, so that the observed titration curves correspond to salt bridge free E28 and D29. This interpretation also explains the relative large amplitude of the chemical shift observed for D29.

Conformational flexibility

The analysis made above is in accord with the opinion that the conformational flexibility of the side chains has a dominant role in the ionization behaviour of proteins. The combination of NMR solution structures and high-resolution X-ray structures may provide such information, as is in the case of K25. However, it is occasional and incomplete, mainly owing to restrictions such as crystal contacts or populations of conformations which are probably favourable only in the crystal state. NMR models, being an alternative source of conformers, suffer from the disadvantage that the side-chain conformations are usually not very well defined.

The NMR solution structure of RNase T_1 provides a good opportunity to evaluate the influence of a conformational variety on the ionization behaviour of the titratable groups. We have calculated the ionization of the individual titratable groups for the 34 best NMR models available in the Protein Data Bank (entry 1YGW) (Pfeiffer et al. 1997). Typical results are illustrated in Fig. 5. One can distinguish a small set of residues, whose pK_a values change in a relatively narrow interval (less than 1.5 in Fig. 5a). These groups (Y4, Y11, Y24, E31, Y42, Y56, Y57, and D66) are either practically non-titratable in the physiologically relevant pH range or well exposed to the solvent in all structures. As a result, these groups interact weakly with the protein charge multipole. The majority of titratable sites, however, are rather sensitive to a conformational variance of the NMR models and the pK_a variation reaches 5.0 pH units (Fig. 5b). The groups with a complex titration, such as H27, belong to this set as for many conformers the complexity is conserved. The main reason for the large variation of the calculated pK_a values is the difference in solvent exposure of the titratable groups. This test clearly illustrates the sensitivity of ionization equilibria in proteins to the desolvation energy, an effect pointed out previously by Warshel et al. (1984).

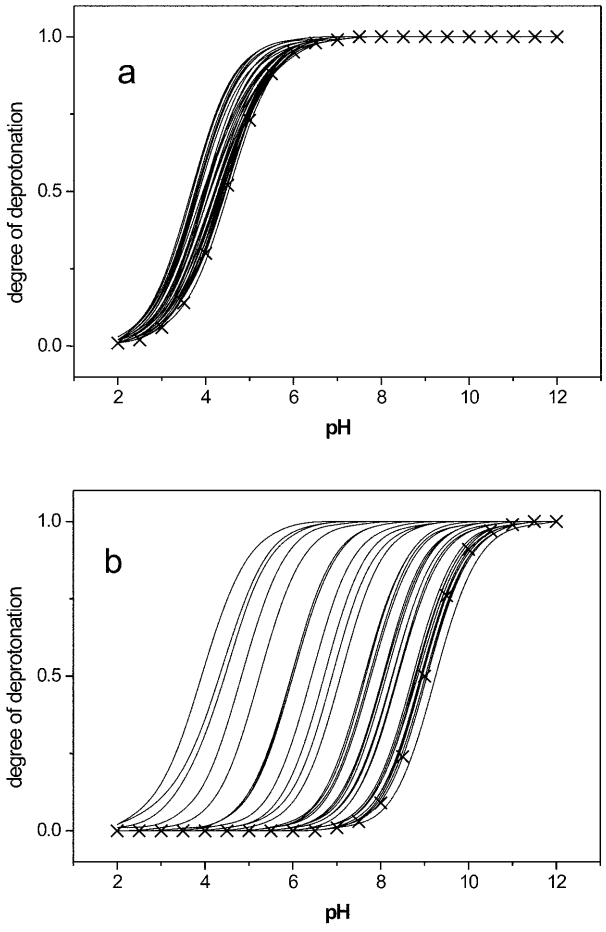

Fig. 5 Calculated titration curves (according to scheme 1) for 34 solution structures (—) and a crystal structure (×) of RNase T_1 for E31 (**a**) as a representative of the sites, which show similar ionization properties in all structures, and the N-terminal amino group (**b**) as illustration of the dependence of the pK_a on conformational flexibility for most of the titratable sites. Groups showing an unusual titration conserve the peculiarity in the shape of their titration curves in most of the structures

It must also be noted that pH-dependent chemical shifts were observed for a number of non-titratable groups with a midpoint at pH 3.6–3.9 (see preceding paper). As far as monitoring nuclei are sensitive to changes of the environment in general, the observed dependence can be attributed to a global conformational transition of the molecule with an apparent midpoint in the pH region between 3.6 and 3.9. The pK_a value of E58 was calculated on the basis of a structure corresponding to pH 7, where the deprotonated state of this residue is well stabilized. The presumed conformational transition may be coupled with the ionization of this residue, an effect which is omitted in the current considerations.

Comments on the electrostatic calculations

The fact that the weakly interacting sites can be predicted by electrostatic calculations is not surprising. It is

also known that the ionization of groups with extremely shifted pK_a values is not always theoretically reproduced with the desired accuracy. The introduction of factors such as the alteration of proton location (Alexov and Gunner 1997) and conformational flexibility, both discussed earlier by Spassov and Bashford (1999), is necessary, which, however, increases the complexity of the problem. In this work, we tried to reduce this complexity by separating the weakly and strongly interacting sites.

One feature that comes out from the theoretical calculations is that the strongly interacting groups may not follow a sigmoidal-shaped titration curve. This is apparent in the calculated ionization curve of H27 (Fig. 2). Bashford and Gerwert (1992) have already discussed such a titration behaviour. Although their theoretical observation was for a pH range above 17, these authors pointed out that ionization curves with multiple inflections could be observed at physiologically relevant pH. Also, Karshikoff et al. (1994) have shown that strongly interacting groups may behave as a single site with an apparent pK_a rather different from that expected for these groups in proteins. In the present paper we illustrate that complex, non-sigmoidal-shaped titration curves may indeed be observed.

Multi-sigmoidal curves are often experimentally observed by NMR and other spectroscopic methods (McNutt et al. 1990; Quirk and Raines 1999; Sackett et al. 1999). The most plausible interpretation of such curves is that they reflect the ionization of two or more titratable groups. Similarly, the pH dependence of the chemical shift of the $^{13}C^{\epsilon 1}$ resonance of H27, reported in the preceding paper, indicates two pK_a values corresponding to E82 (pK_a 3.4) and to H27 (pK_a 7.1). The calculated titration curve rather well reproduces the experimental one, displaying two inflections at pH 3 and pH 7; however, it represents the proton occupancy on $N^{\delta 1}$ of this residue as a function of pH. The stepwise deprotonation may result from the basic assumption of the model, namely that the protein conformation is rigid, i.e. neither side-chain flexibility nor possible conformational changes during titration are taken into account. As mentioned above, a global conformational transition at pH 3.6–3.9 is suspected, so that the rigid structure used in the calculations does not represent a complete picture of the site of the deprotonation process. However, it is notable that the calculated titration curves with two inflection points lead to pK_a values which are very close to the experimental pK_a values of the two strongly interacting side chains.

Yang et al. (1993) have shown that a complex ionization with two inflection points occurs when two acidic groups are strongly interacting. Applying a similar analysis, the same effect can easily be shown for acid-base couples if the intrinsic pK_a value (in terms of Tanford) of the acidic group is higher than that of the basic group. The calculations based on the X-ray structure showed a high desolvation energy for both H27 and E82, which shifts their intrinsic pK_a values to 3.7 and 6.5, respectively. This energy is compensated mainly by the strong (4.1 kcal/mol) and pH-dependent charge-charge interactions between the two sites, which results in a complex ionization curve.

Acknowledgements This work was financially supported by grant BIO4CT970129 of the IV Biotechnology Programme of the European Community. A.K. thanks Prof. Ladenstein (Department of Biosciences at Novum, Karolinska Institute) for useful discussions.

References

Alexov E, Gunner MR (1997) Incorporating protein conformational flexibility into the calculation of pH-dependent protein properties. Biophys J 74:2075–2093

Alexov EG, Gunner MR (1999) Calculated protein and proton motion coupled to electron transfer: electron transfer form Q_A-Q_B to Q_B in bacterial photosyntetic reaction centers. Biochemistry 38:8253–8270

Bashford D, Gerwert K (1992) Electrostatic calculations of the pK_a values of ionizable groups in bacteriorhodopsin. J Mol Biol 224:473–486

Bashford D, Karplus M (1990) pK_a's of ionizable groups in proteins: atomic detail from a continuum electrostatic model. Biochemistry 29:10219–10225

Berisio R, Lamzin VS, Sica F, Wilson KS, Zagari A, Mazzarella L (1999) Protein titration in the crystal state. J Mol Biol 292:845–854

Engelke J, Rüterjans H (1998) Dynamics of β-CH and β-CH2 groups of amino acid side chains in proteins. J Biomol NMR 11:165–183

Giletto A, Pace CN (1999) Buried, charged, non-ion-paired aspartic acid 76 contributes favorably to the conformational stability of ribonuclease T_1. Biochemistry 38:13379–13384

Halgren TA (1996) Merck molecular force field. II. MMFF94 van der Waals and electrostatic parameters for intermolecular interactions. J Comput Chem 17:520–552

Hamer WJ (1971) Properties of dielectrics. In: Weast RC (ed) Handbook of chemistry and physics, 51st edn. Chemical Rubber, Cleveland, Ohio, p E-67

Iida S, Ooi T (1969) Titration of ribonuclease T_1. Biochemistry 8:3897–3901

Karshikoff A (1995) A simple algorithm for calculation of multiple site titration curves. Protein Eng 8:243–248

Karshikoff A, Spassov V, Cowan RQ, Ladenstein R, Schirmer T (1994) Electrostatic analysis of two porin channels from *E. coli*. J Mol Biol 240:372–384

Kirkwood JG (1934) Theory of solutions of molecules containing widely separated charges with special application to zwitterions. J Chem Phys 2:351–361

Klapper I, Hagstrom R, Fine R, Sharp K, Honig B (1986) Focusing of electric fields in the active site of Cu-Zn superoxide dismutase: effects of ionic strength and amino-acid modification. Proteins Struct Funct Genet 1:47–59

Martinez-Oyanedel J, Choe HW, Heinemann U, Saenger W (1991) Ribonuclease T1 with free recognition and catalytic site: crystal structure analysis at 1.5 Å resolution. J Mol Biol 222:335–352

Matthew JB (1985) Electrostatic effects in proteins. Annu Rev Biophys Biophys Chem 14:387–417

McNutt M, Mullins LS, Raushel FM, Pace CN (1990) Contribution of histidine residue to the conformational stability of ribonuclease T1 and mutant Glu-58→Ala. Biochemistry 29:7572–7576

Mehler EL (1996) Self-consistent, free energy based approximation to calculate pH dependent electrostatic effect in proteins. J Phys Chem 100:16006–16018

Miteva M, Demirev PA, Karshikoff AD (1997) Multiply-protonated protein ions in the gas phase: calculation of the electrostatic interactions between charged sites. J Phys Chem 101:9645–9650

Nakasako M, Takahashi H, Shimba N, Shimada I, Arata Y (1999) The pH-dependent structural variation of complementarity-determining region H3 in the crystal structures of the Fv an fragment from anti-dansyl monoclonal antibody. J Mol Biol 291:117–134

Nicholls A, Honig B (1991) A rapide finite difference algorithm, utilizing successive over-relaxation to solve the Poisson-Boltzmann equation. J Comput Chem 12:435–445

Pfeiffer S, Karimi-Nejad Y, Rüterjans H (1997) Limits of NMR structure determination using variable target function calculations: ribonuclease T_1 a case study. J Mol Biol 266:400–423

Pfeiffer S, Spitzner N, Löhr F, Rüterjans H (1998) Hydration water molecules of nucleotide-free ribonuclease T1 studied by NMR spectroscopy in solution. J Biomol NMR 11:1–15

Quirk DJ, Raines RT (1999) His ... Asp catalytic dyad of ribonuclease A: histidine pK_a values in the wild-type, D121N, and D121A enzymes. Biophys J 76:1571–1579

Sackett DL, Ruvinov SB, Thompson J (1999) N-5-(L-1-carboxyethyl)-L-ornithine synthase: physical and spectral characterization of the enzyme and its unusual low pK_a fluorescent tyrosine residues. Protein Sci 8:2121–2129

Spassov VZ, Bashford D (1999) Multiple-site ligand binding to flexible macromolecules: separation of global and local conformational change and an iterative mobile clustering approach. J Comput Chem 20:1091–1111

Srinivasan J, Trevathan MW, Beroza P, Case DA (1999) Application of a pairwise generalized Born model to proteins and nucleic acids: inclusion of salt effects. Theor Chem Acc 101:426–434

Tanford C, Kirkwood JG (1957) Theory of titration curves. I. General equations for impenetrable spheres. J Am Chem Soc 79:5333–5339

Tanford C, Roxby R (1972) Interpretation of protein titration curves. Application to lysozyme. Biochemistry 11:2192–2198

Ullmann GM, Knapp EW (1999) Electrostatic models for computing protonation and redox equilibria in proteins. Eur Biophys J 28:533–551

Warshel A (1981) Electrostatic basis of structure-function correlation in proteins. Acc Chem Res 14:284–290

Warshel A, Russell ST (1984) Calculations of electrostatic interactions in biological systems and in solutions. Q Rev Biophys 17:283–422

Warshel A, Russell ST, Churg AK (1984) Macroscopic models for studies of electrostatic interactions in proteins: limitations and applicability. Proc Natl Acad Sci USA 81:4785–4789

Warwicker J, Watson NC (1982) Calculation of the electric field potential in the active site cleft due to alpha-helix dipoles. J Mol Biol 157:671–679

Yang A-S, Gunner MR, Sampogna R, Sharp K, Honig B (1993) On the calculation of pK_as in proteins. Proteins 15:252–265